Differential Expression of Group I Metabotropic Glutamate Receptors in Functionally Distinct Hippocampal Interneurons

Johannes A. van Hooft, Raffaella Giuffrida, Maria Blatow, and Hannah Monyer

Neurology University Hospital, Department of Clinical Neurobiology, D-69120 Heidelberg, Germany

Metabotropic glutamate receptors (mGluRs) have been proposed to be involved in oscillatory rhythmic activity in the hippocampus. However, the subtypes of mGluRs involved and their precise distribution in different populations of interneurons is unclear. In this study, we combined functional analysis of mGluR-mediated inward currents in CA1 oriens–alveus interneurons with anatomical and immunocytochemical identification of these interneurons and expression analysis of group I mGluR using single-cell reverse transcription-PCR (RT-PCR). Four major interneuron subtypes could be distinguished based on the mGluR-mediated inward current induced by the application of 100 μM trans-(1*S*,3*R*)-1-aminocyclopentane-1,3-dicarboxylic acid (ACPD) under voltage-clamp conditions and the action potential firing pattern under current-clamp conditions. Type I interneurons responded with a large inward current of ~224 pA, were positive for somatostatin, and the majority expressed both mGluR1 and mGluR5. Type II interneurons responded with an inward current of ~80 pA, contained calbindin, and expressed mainly mGluR1. Type III interneurons responded with an inward current of ~60 pA. These interneurons were fast-spiking, contained parvalbumin, and expressed mainly mGluR5. Type IV interneurons did not respond with an inward current upon application of ACPD, yet they expressed group I mGluRs. Activation of group I mGluRs under current-clamp conditions increased spike frequency and resulted in rhythmic firing activity in type I and II, but not in type III and IV, interneurons. RT-PCR results suggest that activation of mGluR1 in the subsets of GABAergic interneurons, classified here as type I and II, may play an important role in mediating synchronous activity.

Key words: interneuron; metabotropic glutamate receptor; single-cell RT-PCR; in situ *patch clamp; rhythmic activity; hippocampus*

Inhibitory interneurons exert a powerful control over local neuronal circuits by mediating feedforward and feedback inhibition. Because of the large divergence of the output of individual interneurons onto large numbers of principal neurons (Buhl et al., 1994; Sik et al., 1995, Miles et al., 1996), the activity of an individual interneuron can have great impact on the excitability of the local neuronal network (Cobb et al., 1995; Katona et al., 1999). Networks of interconnected interneurons are able to generate synchronous oscillations (Buzsaki and Chrobak, 1995; Whittington et al., 1997). These oscillations are thought to be an electrophysiological substrate for temporal and spatial information processing within and between brain regions during specific behavioral states (Singer, 1993). Although it is recognized that networks of interneurons are capable of providing the cellular substrate, the molecular substrates underlying the induction and maintenance of these synchronous oscillations are obscure. Also, it is not clear which subtypes of GABAergic interneurons are critical for the generation of oscillatory activity. Oscillations in the range of 30–70 Hz (γ frequency) can be evoked in hippocampal slices in vitro by a number of manipulations, including tetanic stimulation or application of agonists for muscarinic acetylcholine receptors (Whittington et al., 1997; Fisahn et al., 1998). In addition, activation of metabotropic glutamate receptors (mGluRs) drives oscillations of inhibitory networks (Whittington et al., 1995; Boddeke et al., 1997). Moreover, the frequency of oscillations is dependent on the degree of slow excitation of interneurons, and it has been suggested that mGluRs may be involved in this slow excitatory drive (Whittington et al., 1995; Traub et al., 1996, 1997).

Here, we show that the slow excitation of oriens–alveus interneurons by the nonselective mGluR agonist trans-(1*S*,3*R*)-1-aminocyclopentane-1,3-dicarboxylic acid (ACPD) is mediated by postsynaptic group I mGluRs. Based on the size of the mGluR-mediated inward current and the action potential firing pattern, four subtypes of interneurons could be distinguished. Using single-cell reverse transcription-PCR (RT-PCR), we show that these different interneuron populations display distinct expression profiles of mGluR1 and mGluR5. Activation of mGluRs on interneurons, which are strongly excited by group I mGluR activation, evokes highly rhythmic action potential firing, and this activity appears to be mediated by mGluR1. Hence, differential expression of mGluR1 and mGluR5 contributes to the functional segregation of interneurons and may serve as a molecular determinant of the degree of slow excitatory input onto interneurons, which may be crucial during distinct oscillatory states.

MATERIALS AND METHODS

Electrophysiology. Wistar rats [postnatal day 14 (P14) to P16] were decapitated, and the brain was quickly removed. Slices (250 μm) of the hippocampus were cut using a vibroslicer (752M; Campden Instruments,

Received Jan. 11, 2000; revised Feb. 28, 2000; accepted Feb. 29, 2000.

This study was supported by Deutsche Forschungsgemeinschaft Grant Mo432/3-1 and the Schilling Foundation to H.M. and a NATO-Science Fellowship to J.A.v.H. M.B. was supported by the Graduate Program of Molecular and Cellular Neurobiology of the University of Heidelberg. We thank Ulla Amtmann for expert technical assistance and Peter Jonas, Richard Miles, Roger Traub, Wytse Wadman, and Bill Wisden for helpful comments on this manuscript.

Correspondence should be addressed to Hannah Monyer, Neurology University Hospital, Department of Clinical Neurobiology, Im Neuenheimer Feld 364, D-69120 Heidelberg, Germany. E-mail: monyer@mpimf-heidelberg.mpg.de.

Dr. van Hooft's present address: Institute of Neurobiology, University of Amsterdam, Kruislaan 320, NL-1098 SM Amsterdam, The Netherlands.

 0270-6474/00/203544-08$15.00/0

Loughborough, UK), and the slices were allowed to recover for at least 1 hr at 31°C in standard Ringer's solution containing (in mM): NaCl 125, KCl 2.5, $CaCl_2$ 2, $MgCl_2$ 1, $NaHCO_3$ 25, NaH_2PO_4 1.25, and glucose 25, continuously bubbled with 95% O_2–5% CO_2. Patch pipettes were pulled from boroscilicate glass and had a resistance of 1.5–3 MΩ when filled with internal solution containing (in mM): KCl 140, $MgCl_2$ 2, EGTA 5, and Na-HEPES 10, pH 7.3 with KOH. Interneurons in the alveus and stratum oriens of the CA1 area were visualized using infrared differential interference contrast videomicroscopy (Stuart et al., 1993). Whole-cell recordings were made using an EPC9 patch-clamp amplifier and PULSE software (HEKA Electronik GmbH, Lambrecht, Germany). The series resistance ranged from 7 to 20 MΩ. During the recording, slices were kept submerged and were continuously superfused with Ringer's solution at room temperature (20–22°C). After recording of action potentials, cells were voltage clamped (V_h of −80 mV). Drugs were applied via a capillary positioned close to the surface of the slice. Controls with Ringer's solution containing phenol red showed that stratum oriens, stratum pyramidale, and the proximal part of stratum radiatum were efficiently superfused. In some experiments, drugs were applied by bath perfusion. Signals were filtered at 1–5 kHz and sampled at 2–10 kHz. Signals were stored on disk, and off-line analysis was performed using the program PULSEFIT (HEKA Electronik GmbH) and IGOR (WaveMetrics Inc., Lake Oswego, OR). All results are expressed as mean ± SD of *n* independent experiments and compared using Student's *t* test.

Single-cell RT-PCR. For single-cell RT-PCR analysis (Lambolez et al., 1992; Monyer and Jonas, 1995) of mGluR1 and mGluR5 expression, the cytoplasm of interneurons was aspirated into patch pipettes, pulled from autoclaved boroscilicate glass (resistance of 1.5–2.5 MΩ, filled with autoclaved internal solution), by gentle suction under visual control after the electrophysiological recordings had been made. The harvested material was subsequently expelled into an autoclaved tube containing desoxyribonucleoside triphosphates, dithiothreitol, ribonuclease inhibitor, and Superscript reverse transcriptase, and incubated for 1 hr at 37°C. Two rounds of PCR amplification were performed. The template for the second PCR was 5 μl of the first PCR. The primer pairs were chosen to amplify both mGluR1 and mGluR5 but not any of the other mGluR receptor subtypes. Control PCR experiments using different ratios of mGluR1 and mGluR5 cDNA indicated that the primer pairs did not preferentially amplify either mGluR1 or mGluR5 (data not shown). For the first PCR, the 5′ primer was GAAGCCCAGATTCATGAGCGC (located 2088 bp downstream from the start codon), and the 3′ primer was AAACATGCA(AC)CCCAGGGCCAC (located 2493 bp downstream from the start codon). For the second PCR, the same 5′ primer was used, together with a nested 3′ primer: GTGATGAT(CT)TTGTAGTTGCT (located 2441 bp downstream from the start codon). The primer pairs were intron-overspanning to distinguish amplification of cDNA from amplification of genomic DNA in case the nucleus was harvested. The PCR conditions were the same for both amplification rounds; after a hot start at 94°C for 5 min, 35 cycles (94°C for 30 sec; 53°C for 30 sec; 72°C for 40 sec) and an elongation step at 72°C for 10 min were performed. The presence of mGluR1 and/or mGluR5 was determined by Southern blot using subtype-specific radiolabeled probes [CATGCCCATTTTGTCCTACCCG (located 2190 bp downstream from the start codon for mGluR1) and GGATATAATGCATGACTATCCA (located 2148 bp downstream from the start codon for mGluR5)]. The washing conditions were 0.2× SSC at 50°C. A signal was considered positive when both the ethidium bromide-stained gel and the Southern blot gave a positive signal. Controls for artifacts during harvesting and amplification were performed during each experiment. For each group, the success rate of amplification was 75%. We do not conclude that the other 25% of the cells do not express mGluRs. The most likely explanation for what we think are "false negatives" is insufficient amounts of harvested material and/or loss of it during the expelling procedure. In previous studies in which AMPA and NMDA receptor subunits were amplified in interneurons, a similar efficiency was obtained.

Biocytin filling, immunostaining, and in situ *hybridization.* Cells were filled with biocytin (1–4 mg/ml, dissolved in internal solution) during the experiment. Subsequently, the slice was fixed overnight in 4% paraformaldehyde. For reconstruction of the cells by camera lucida, biocytin was visualized using an avidin-HRP reaction (ABC Elite peroxidase kit; Vector Laboratories, Burlingame, CA) according to the instructions of the manufacturer. For double labeling of functionally characterized interneurons, fixed slices were embedded in 4% agar and resliced at 50–60 μm. Slices were transferred in TBS and permeabilized for 30 min in TBS with 0.4% Triton X-100. This was followed by a preincubation in TBS containing 4% normal goat serum (NGS). Sections were then incubated overnight at 4°C in TBS containing 0.1% Triton X-100, 2% NGS with either mouse monoclonal anti-parvalbumin (1:1000; Sigma-Aldrich, Deisenhofen, Germany), or mouse monoclonal anti-calbindin (1:200; Sigma-Aldrich) or rabbit polyclonal anti-calretinin (1:1000; Swant, Bellinzona, Switzerland) primary antibodies. On the following day, slices were washed in TBS and incubated for 2 hr with the appropriate secondary antibody, conjugated to Texas Red, together with FITC-conjugated avidin to stain the biocytin-filled cell. Subsequently, slices were mounted in Mowiol, and cells were visualized using immunofluorescence microscopy with appropriate filter sets for Texas Red and FITC.

An antibody of comparable quality for somatostatin was not available at the time the experiments were performed. Therefore, the expression of somatostatin was investigated using a nonradioactive *in situ* hybridization labeling method. A 340 bp DNA fragment encompassing 60 bp of the 5′ untranslated region and the first 280 bp of the open reading frame of the rat preprosomatostatin sequence (Montminy et al., 1984) was obtained by PCR with rat hippocampal cDNA as a template and subcloned into the pBluescript SK− vector (Stratagene, La Jolla, CA). *In vitro* transcription and digoxigenin labeling of the riboprobe and nonradioactive *in situ* hybridization using the digoxigenin-labeled riboprobe was performed as described previously (Catania et al., 1995). After *in situ* hybridization, sections were processed for biocytin detection with FITC-conjugated avidin as described above. The specificity of the antibodies and the riboprobe were documented on whole brain sections and were identical with previously described expression patterns of these subsets of GABAergic interneurons (data not shown).

Drugs. ACPD, tetrodotoxin (TTX), D-2-amino-5-phosphonopentanoic acid (D-AP-5), and picrotoxin were purchased from Research Biochemicals (Natick, MA); biocytin was purchased from Sigma; CNQX, L-2-amino-4-phosphonobutyric acid (L-AP-4), (*RS*)-α-methyl-4-carboxyphenylglycine (MCPG), (*S*)-4-carboxyphenylglycine (*S*-4-CPG), (*RS*)-3,5-dihydroxyphenylglycine (DHPG), and (*RS*)-α-methyl-4-phosphonophenylglycine (MPPG) were purchased from Tocris Cookson (Bristol, UK). All drugs were prepared as concentrated stock solutions and stored at −20°C. CNQX was dissolved in dimethylsulphoxide, MCPG, MPPG, and *S*-4-CPG were dissolved in equimolar NaOH, and all other drugs were dissolved in water.

RESULTS

Oriens–alveus interneurons respond differentially to mGluR activation

Local perfusion of the nonselective mGluR agonist ACPD (100 μM; in the presence of 1 μM TTX) under whole-cell voltage-clamp conditions evoked an inward current in 79.4% ($n = 141$) of the interneurons tested. The ACPD-evoked inward current activated within 5–10 sec after application of the agonist (Fig. 1*A*). The presence of the ion current was related to the presence of the agonist; upon removal of the agonist, the ion current returned to baseline. It has previously been reported that bath perfusion of ACPD results in an oscillatory inward current with long latency (~1 min) and slow time course in a subset of interneurons (McBain et al., 1994). Similar ion currents could be evoked using bath application of 100 μM ACPD under the conditions used in our experiments (Fig. 1*A*).

The size of the ACPD-induced inward current differed between interneurons (Fig. 1*B*). On the basis of this difference and the difference in their action potential firing pattern, the interneurons were classified into four types (Fig. 1*C*). In type I interneurons, application of 100 μM ACPD resulted in an inward current of 224 ± 76 pA ($n = 48$). These interneurons were large, with horizontally located cell bodies at the border of stratum oriens and the alveus. Injection of a 150 pA current under current-clamp conditions evoked regular action potential firing at a rate of 26.6 ± 5.5 Hz ($n = 48$). Type II interneurons displayed similar regular action potential firing (30.6 ± 7.1 Hz, $n = 26$). However, these interneurons responded with a small inward current of 80 ± 30 pA ($n = 26$) upon application of 100 μM ACPD. These interneurons were located throughout stratum oriens. The

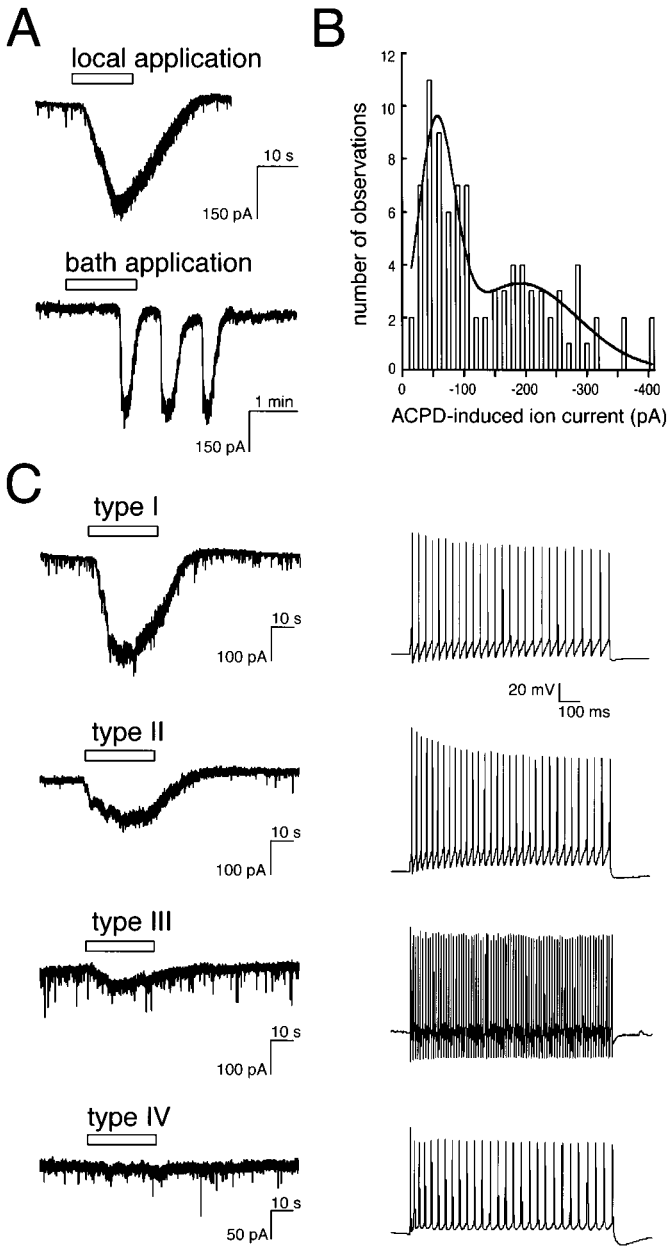

Figure 1. Distinct interneurons respond differentially to application of 100 μM ACPD. *A*, Bath application of 100 μM ACPD evoked a slow, oscillatory inward current in voltage-clamped stratum oriens–alveus interneurons. Local application of ACPD evoked an inward current with similar amplitude but with faster time course. *B*, Histogram of the amplitudes of ACPD-evoked inward currents in stratum oriens–alveus interneurons ($n = 96$). Interneurons not responding to application of ACPD have not been included in the histogram. Gaussian curves were drawn to illustrate the existence of two populations. *C*, Inward currents evoked with 100 μM ACPD and evoked action potential firing (150 pA, 1 sec) in the four types of interneurons. All ACPD-induced currents were recorded in the presence of 1 μM TTX.

third type of interneuron also responded with a small response of 60 ± 21 pA ($n = 23$) upon application of 100 μM ACPD. The responses in these cells occasionally (8 of 23 cells) oscillated (0.02–0.05 Hz). These interneurons were located in stratum oriens, close to stratum pyramidale, but they did not represent ectopically located pyramidal neurons and differed from type II interneurons as indicated by their characteristic high-frequency action potential firing (Fig. 1*C*, Table 1). The last type of interneuron did not respond to the application of 100 μM ACPD. The action potentials of these neurons displayed a small afterhyperpolarization compared with the other types of interneurons (Table 1). Somata of these interneurons were located throughout stratum oriens. Detailed electrophysiological characteristics of the interneuron subtypes are summarized in Table 1.

Immunocytochemistry, *in situ* hybridization, and reconstruction of the interneurons were performed to correlate the four types of interneurons to previously described interneurons. Based on morphological criteria and the expressed neurochemical markers, type I and III GABAergic neurons comprised a homogenous cell population, which contrasted with type II and type IV interneurons that were heterogenous.

Type I interneurons had large horizontally oriented cell somata located at the border of stratum oriens and the alveus, indicating that these cells were most likely identical with the previously described somatostatin-positive oriens-lacunosum moleculare (O-LM) cells (Freund and Buzsáki, 1996). Reconstruction of type I interneurons revealed their horizontally oriented dendritic tree in stratum oriens and their axonal arborizations in stratum lacunosum-moleculare ($n = 5$) (Fig. 2*A*), and *in situ* hybridization for somatostatin showed that four of four cells were indeed positive for somatostatin (Fig. 2*B*). Whereas in most brain regions somatostatin-positive cells only seldom contain calbindin as well, in stratum oriens of the hippocampus, the majority of somatostatin-positive cells are also positive for calbindin (Freund and Buzsáki, 1996). Our results are in agreement with these findings, because three of five type I interneurons were calbindin-positive (data not shown).

Type III interneurons were putative basket or chandelier cells as judged by their location close to stratum pyramidale and their characteristic high-frequency firing pattern. Reconstruction of type III interneurons confirmed their identity; the dendritic tree runs vertically from stratum oriens to stratum radiatum, and the axonal arborizations are confined to stratum pyramidale ($n = 6$) (Fig. 2*A*). These interneurons have been shown to be parvalbumin-positive (Freund and Buzsáki, 1996). Immunostaining on four cells confirmed that these interneurons are parvalbumin-positive basket or chandelier cells (Fig. 2*C*).

Morphological and immunochemical characterization of type II and IV interneurons revealed a complex picture when five interneurons of each type were reconstructed. Figure 3 shows that the axonal and dendritic distribution pattern is highly variable. The five type II interneurons were all calbindin-positive (data not shown). The heterogeneity of type IV interneurons also extended to the expression of neurochemical markers; two of six cells were found to be positive for calretinin, and two of five cells contained calbindin (data not shown).

The ACPD-induced inward current is mediated by group I mGluRs

ACPD-induced inward currents in oriens–alveus interneurons do not depend on fast synaptic transmission (McBain et al., 1994). In concordance with this finding, Figure 4*A* shows that the ACPD-induced inward current is resistant to 1 μM TTX. In addition, the ACPD-induced inward current persists in the presence of a cocktail of antagonists of NMDA (D-AP-5), AMPA (CNQX), $GABA_A$ (picrotoxin), and group II/III mGlu (MPPG) receptors (Fig. 4*A*). Thus, the ACPD-induced inward current is mediated by postsynaptic mGluRs. Similar inward currents could be evoked with 100 μM DHPG, a selective group I mGluR agonist (Fig. 4*B*).

Table 1. Summary of the passive and active electrophysiological properties of types I, II, III, and IV interneurons

	V_m (mV)	Evoked spike frequency (Hz)	Spike adaptation ratio	AHP amplitude (mV)	Capacitance (pF)	R_{input} (MΩ)	*n*
Type I	−55.8 ± 5.2	26.6 ± 5.5	1.16 ± 0.07	18.8 ± 2.9	63.4 ± 22.4*	382.9 ± 94.7	53
Type II	−55.0 ± 6.4	30.6 ± 7.1	1.22 ± 0.09	19.9 ± 3.7	43.4 ± 24.8	365.0 ± 73.1	32
Type III	−54.7 ± 4.8	56.0 ± 8.2**	1.05 ± 0.04**	18.5 ± 3.9	44.5 ± 16.4	308.9 ± 66.9	27
Type IV	−57.1 ± 5.4	25.6 ± 6.7	1.19 ± 0.12	8.3 ± 3.1**	54.7 ± 15.9	351.7 ± 89.9	29

The evoked spike frequency was determined by injecting a 150 pA current for 1 sec, which evoked near-maximum spiking frequency in all interneuron subtypes. The spike adaptation ratio was determined by dividing the amplitude of the first spike during this period of 1 sec by the amplitude of the last spike. The afterhyperpolarizing (AHP) amplitude was determined from a spontaneous spike relative to resting V_m. Asterisks indicate significant differences with the other groups (*$p < 0.01$; **$p < 0.001$).

Moreover, the ACPD-evoked inward current could be reversibly blocked by the nonselective mGluR antagonist MCPG and the selective group I antagonist *S*-4-CPG (Fig. 4*C*). Application of the selective group III mGluR agonist L-AP-4 (300 μM) did not result in an inward current in all types of interneurons examined (data not shown). These results indicate that the ACPD-induced inward current is mediated by postsynaptic group I mGluRs. It is of note that, apart from the size of the 100 μM ACPD-evoked inward current, the ratio of the amplitudes of inward currents evoked with ACPD and DHPG differed between interneuron types (Fig. 4*B*). Thus, whereas the ACPD- and DHPG-evoked inward current amplitudes are approximately equal in type I interneurons, in type III interneurons, the DHPG-evoked inward current amplitude is ~2.5 times larger than that of ACPD (Fig. 4*B*). This suggests a differential contribution of group I mGluRs (mGluR1 and mGluR5) to the ACPD-evoked response in different interneuron types.

mGluR1 and mGluR5 are differentially expressed in oriens–alveus interneurons

Because of the lack of selective antagonists, it is difficult to assess the contribution of mGluR1 and/or mGluR5 to the ACPD-induced inward current. Therefore, a single-cell RT-PCR study was performed in which the expression of mGluR1 and/or mGluR5 mRNA was examined in functionally characterized interneurons. Figure 5*A* shows an example of an ethidium bromide-stained gel with PCR products obtained from the four types of interneurons. Southern blot analysis of the gel shown in Figure 5*A* with labeled mGluR1- and mGluR5-specific oligonucleotide probes is shown in Figure 5*B*. The majority of type I interneurons, responding with a large inward current upon ACPD application, express both mGluR1 and mGluR5. In contrast, interneurons, which display a small ACPD-evoked inward current, preferentially express mGluR1 (type II) or mGluR5 (type III). Type IV interneurons, which do not respond to the application of ACPD, do express group I mGluRs, with 30.8% of the neurons expressing mGluR5 and 61.5% expressing both mGluR1 and mGluR5 (Fig. 5*C*).

Activation of mGluRs induces rhythmic firing in type I and II, but not in type III and IV, interneurons

We examined the effects of activation of group I mGluRs on the spike activity of the interneuron subtypes. Figure 6*A* shows stretches of spike activity recorded from a type I and a type III interneuron under control conditions and during application of 100 μM ACPD in the presence of a cocktail of blockers of synaptic transmission (D-AP-5, CNQX, picrotoxin, and MPPG; compare with Fig. 4*A*). The spike activity of the type III interneuron is hardly changed by ACPD (control, 4.6 ± 0.7 Hz; ACPD, 4.3 ± 1.4 Hz; $n = 4$). However, the spike frequency of the

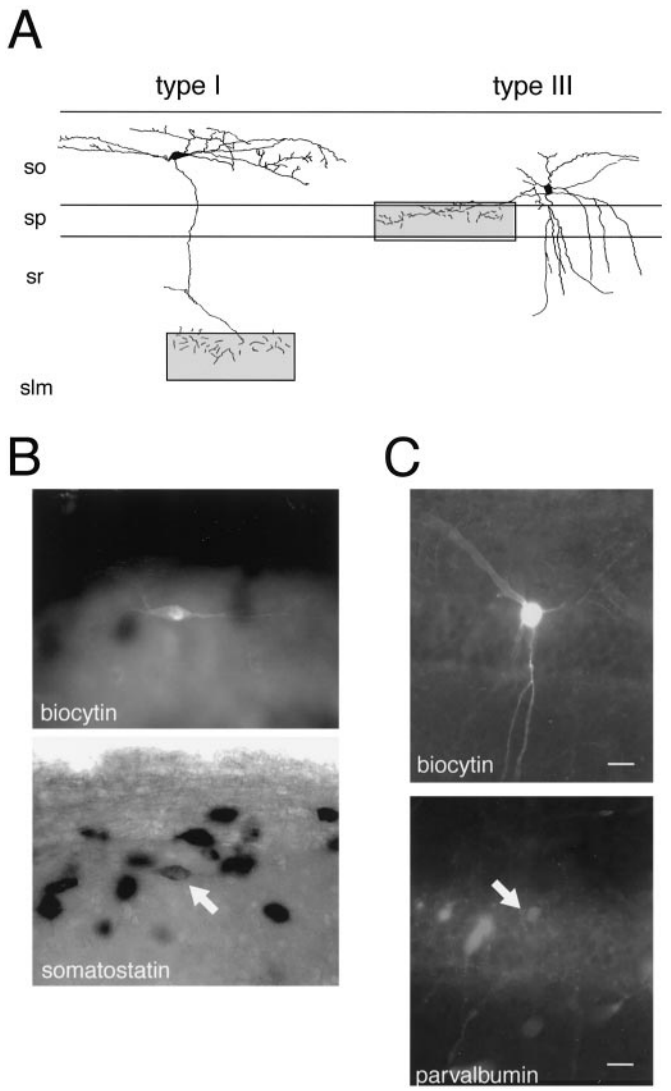

Figure 2. Type I and type III interneurons are O-LM cells and basket cells, respectively. *A*, Camera lucida reconstruction of functionally characterized, biocytin-filled type I and type III interneurons. *Gray boxes* indicate axonal arborization zones. *B*, Biocytin-filled interneuron, stained with avidin-FITC and *in situ* hybridization for somatostatin. *Arrow* indicates the biocytin-filled cell. *C*, Biocytin-filled interneuron, stained with avidin-FITC and immunostaining for parvalbumin on the same cell. Scale bars, 20μm.

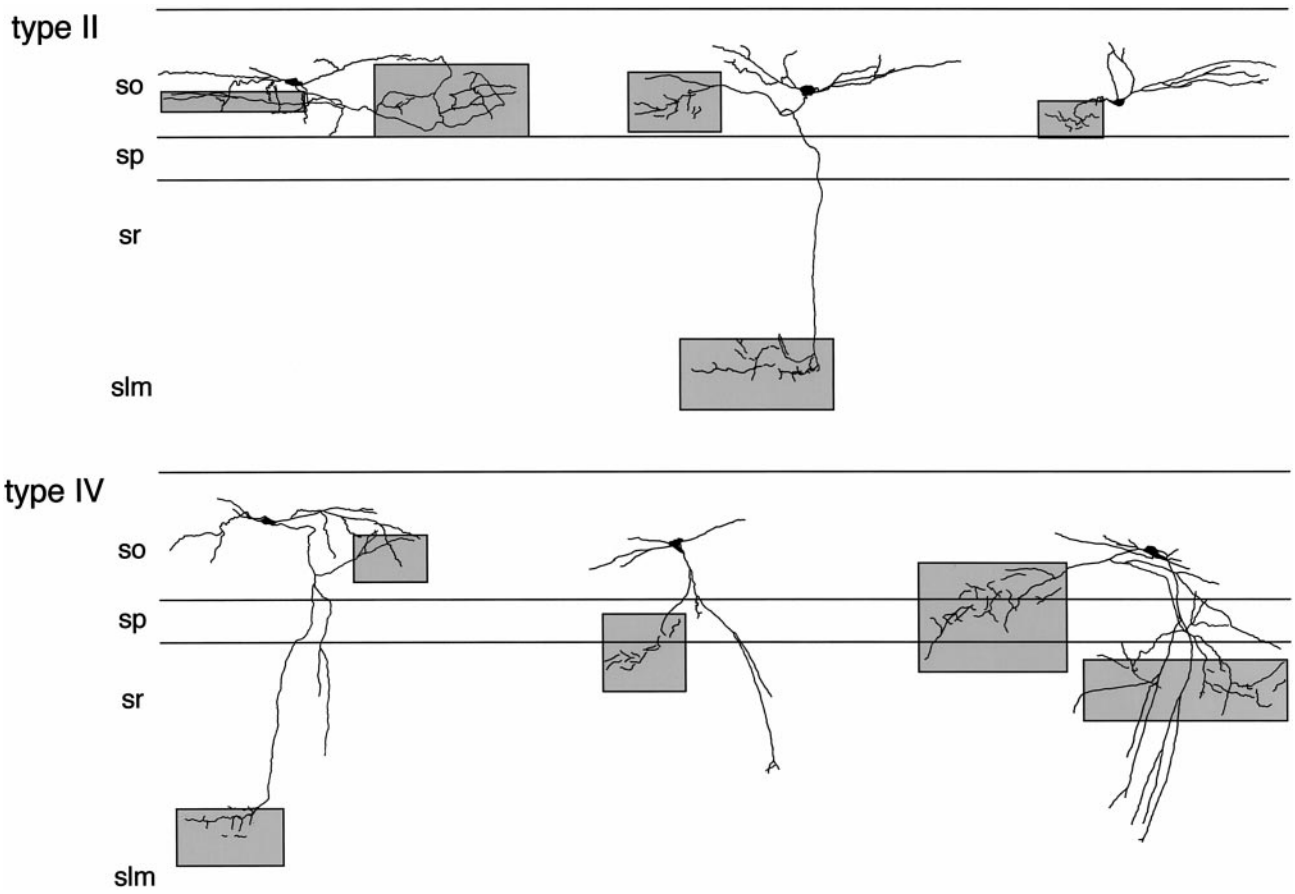

Figure 3. Type II and type IV interneurons represent a heterogeneous population of interneurons. Camera lucida reconstructions of functionally characterized, biocytin-filled interneurons are shown. *Gray boxes* indicate axonal arborization zones.

type I interneuron is increased from 2.4 ± 0.4 to 17.8 ± 4.4 Hz ($n = 4$). Figure 6*B* summarizes the change in spike frequency induced by ACPD in the four interneuron subtypes. Apart from the increase in spike frequency, the type I interneuron displays a highly rhythmic spiking pattern, in contrast to the type III interneuron (Fig. 6*A*). This is more clearly illustrated in Figure 6*C*, which shows autocorrelograms of stretches of spike activity as shown in Figure 6*A*. Type I and II interneurons display a highly rhythmic spiking pattern during application of ACPD, whereas the spiking pattern of type III and IV interneurons is not affected.

DISCUSSION

In this study, we classified oriens–alveus interneurons into four subtypes. This classification is based on the size of the ACPD-induced inward current and the action potential firing pattern. Type I interneurons are located at the oriens–alveus border and have large, horizontally located cell bodies. Their dendritic trees run horizontally, and their axons run vertically toward stratum lacunosum-moleculare (Fig. 2*A*). These interneurons contain somatostatin (Fig. 2*B*). Therefore, these interneurons appear identical to the horizontal O-LM cells (Freund and Buzsáki, 1996; Katona et al., 1999). Type III interneurons have vertically oriented dendritic trees, and their axons terminate exlusively in stratum pyramidale (Fig. 2*A*). Together with the characteristic high-frequency spiking pattern (Fig. 1*C*) and the immunoreactivity for parvalbumin (Fig. 2*C*), these interneurons are putative basket or chandelier cells (Freund and Buzsáki, 1996). Type II and type IV interneurons represent a heterogeneous population of cells. The orientation of the dendritic trees, as well as the axonal arborization zones, varied considerably (Fig. 3). Type II interneurons are immunoreactive for calbindin. For type IV interneurons, immunoreactivity was found for both calbindin and calretinin, two markers that have been shown not to colocalize in the hippocampus (Freund and Buzsáki, 1996). These interneurons might include bistratified and trilaminar cells, which are often calbindin-positive, as well as interneurons specifically innervating other interneurons, which are often calretinin-positive (Freund and Buzsáki, 1996).

We did not classify the interneurons based on all available physiological and morphological criteria; there is not always a direct correlation between morphological, physiological, and molecular parameters, suggesting that hippocampal interneurons cannot easily be segregated into a few well defined groups (Kawaguchi, 1997; McMahon et al., 1998; Parra et al., 1998). A close correlation of certain criteria, as shown here for type I and type III interneurons, does not exclude the possibility that these subtypes can be further subdivided if additional criteria are considered.

It has been shown before that bath application of ACPD evokes large, oscillatory inward currents in a subset of oriens–alveus interneurons, which innervate stratum lacunosum-moleculare (McBain et al., 1994; Woodhall et al., 1999). In addition, another subset of interneurons, which innervate somata and proximal dendrites of CA1 pyramidal neurons, respond with a small, non-oscillatory inward current upon bath application of

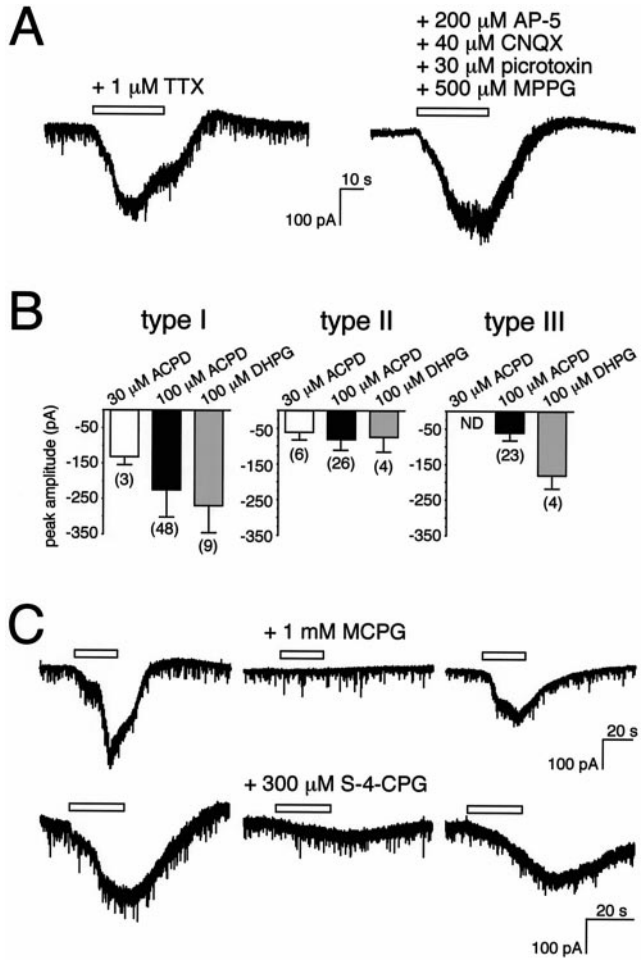

Figure 4. The ACPD-induced inward current is mediated by postsynaptic group I mGluRs. *A*, Inward currents evoked with 100 μM ACPD in a type I interneuron in the presence of 1 μM TTX (*left*) and after 2 min of superfusion with a cocktail of antagonists of NMDA receptors (AP-5), AMPA receptors (CNQX), $GABA_A$ receptors (picrotoxin), and presynaptic mGluRs (MPPG) (*right*). *B*, Summary of the amplitudes of the inward currents evoked with ACPD (30 and 100 μM) and the selective group I mGluR agonist DHPG (100 μM) in type I, II, and III interneurons. The *number* in parentheses indicates the number of cells (*ND*, not determined). *C*, The ACPD-evoked inward current in a type I interneuron is completely blocked after 2 min of superfusion with 1 mM of the nonselective mGluR antagonist MCPG. The selective group I mGluR antagonist *S*-4-CPG (300 μM) blocks the ACPD-evoked inward current to 19.0 ± 1.7% ($n = 3$) of control.

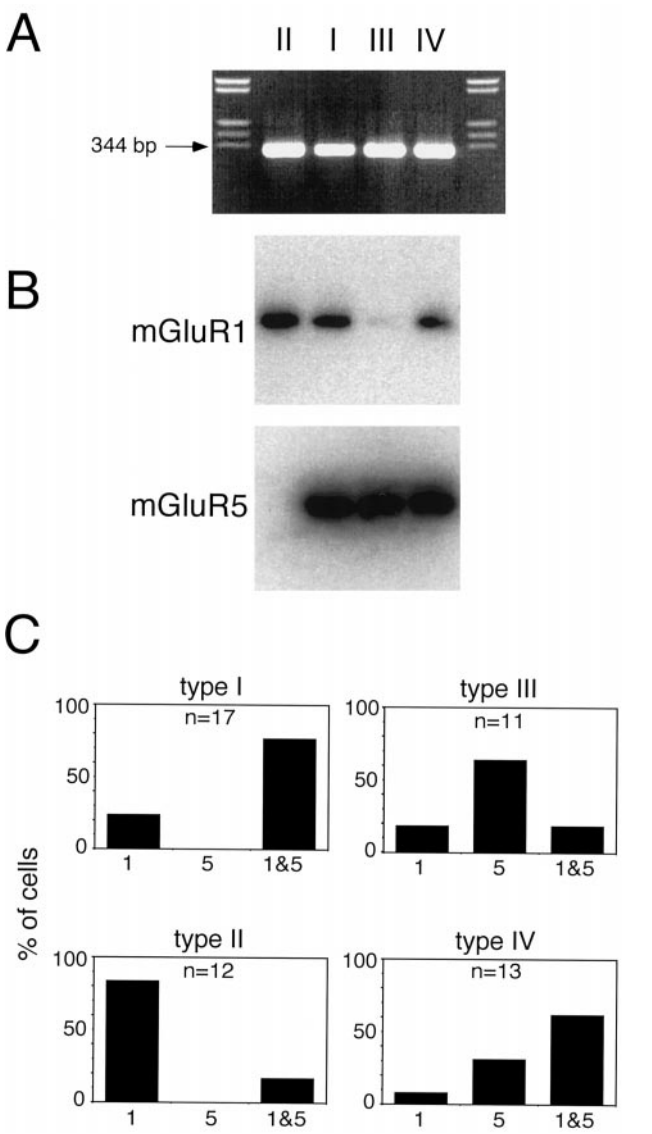

Figure 5. Single-cell RT-PCR analysis of the presence of mGluR1 and mGluR5 mRNA in oriens–alveus interneurons. *A*, Ethidium bromide-stained gel of PCR products obtained from the four different cell types, as indicated *above* the *panel*. The *arrow* indicates the expected size of the PCR product (344 bp). *B*, Southern blot of the gel shown in *A*, hybridized with mGluR1- and mGluR5-specific oligonucleotide labeled probes. *C*, Summary of the single-cell RT-PCR results for the four different cell types. *Bars* represent the number of cells positive for mGluR1, mGluR5, or both mGluR1 and mGluR5, expressed as percentage of the total number of cells analyzed.

ACPD (McBain et al., 1994). These two subsets of interneurons appear identical to type I and type III interneurons. In the present study, no oscillatory currents were observed in type I interneurons; instead, type III interneurons occasionally showed oscillatory currents (8 of 23 cells). However, the "discrepancy" between our and previous results is merely caused by the difference in the agonist application; when bath application of ACPD was used instead of fast local application, oscillatory inward currents were observed in type I interneurons (Fig. 1*A*). It is an interesting observation that type I interneurons exhibit a differential response (large inward current vs oscillatory current) that is dependent on the mode of activation (short vs prolonged activation). However, it is premature to speculate on whether and when the different modes of mGluR1 activation occur *in vivo* and what the functional consequences might be.

Type IV interneurons do not respond with an inward current upon application of ACPD or DHPG (Fig. 1*C*). However, they do express group I mGluRs (Fig. 5*C*). Group I mGluRs are G-protein-coupled receptors, and activation results in release of Ca^{2+} from intracellular stores via an inositol triphosphate/Ca^{2+} signal transduction mechanism (Carment et al., 1997; Nakanishi et al., 1998). It has been suggested that the molecular basis of the inward currents evoked by activation of mGluRs is an electrogenic Na^{+}–Ca^{2+} exchanger that is activated upon release from intracellular Ca^{2+} (Staub et al., 1992; McBain et al., 1994; Lee and Boden, 1997). Hence, one possible explanation for the nonresponsiveness of type IV interneurons upon mGluR activation could reside in the absence or the later maturation of the effector

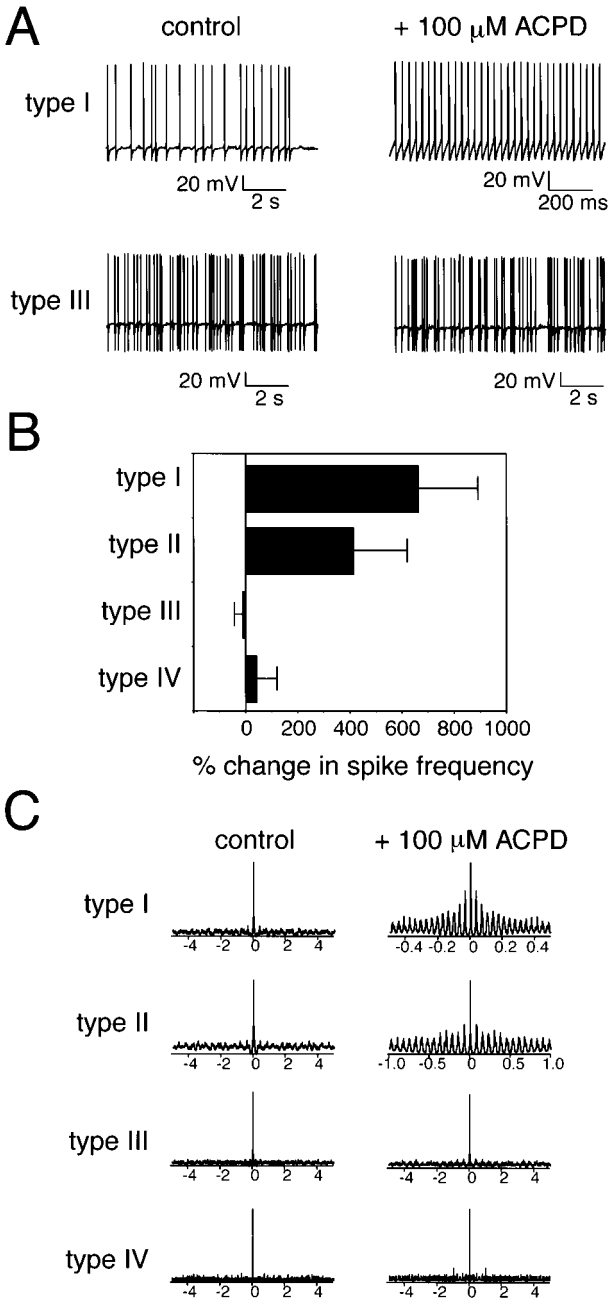

Figure 6. Activation of group I mGluRs induces rhythmic action potential firing in type I and II, but not in type III and IV, interneurons. *A*, Spontaneous action potentials recorded from a type I and type III interneuron in the absence and presence of 100 μM ACPD. Note that the spike frequency of the type I interneuron is increased. *B*, Summary of the change in spike frequency in the presence of 100 μM ACPD. The values for type III and IV interneurons (-10 ± 30 and $40 \pm 80\%$, respectively; $n = 4$) are not significantly different from zero ($p > 0.05$). *C*, Autocorrelograms of stretches of action potential firing, as shown in *A*, recorded under control conditions and 10 sec after application of 100 μM ACPD.

molecule (e.g., Na^+–Ca^{2+} exchanger) in these interneurons. Alternatively, mGluRs expressed by type IV interneurons may be located presynaptically.

The distribution of mGluR1 and mGluR5 in the subtypes of interneurons, as assessed by single-cell RT-PCR (Fig. 5*C*), corroborates and extends previous observations. Thus, large horizontal O-LM cells (type I) had been shown to express high levels of mGluR1 protein (Baude et al., 1993). In another *in situ* hybridization study, mGluR1 expression was found in somatostatin-positive (here type I) but not in parvalbumin-positive (here type III) interneurons, whereas mGluR5 expression was detected both in somatostatin- and parvalbumin-positive interneurons (Kerner et al., 1997). However, the coexpression of mGluR1 and mGluR5 at the single-cell level has not been analyzed so far. The RT-PCR data reveals a complex picture, yet a distinct expression profile is apparent for each of the four interneuron subtypes; the majority of type I and type IV interneurons coexpress mGluR1 and mGluR5. This contrasts with the preferential expression of mGluR1 in type II interneurons and of mGluR5 in type III interneurons.

There is a remarkable difference of the response in the interneuron subtypes with regard to their action potential firing induced by mGluR activation. Inspection of the mGluR expression profiles permits the conclusion that this activity must be mediated by the mGluR1 receptor. Thus, there is a clear-cut difference between interneuron subtypes that exhibit rhythmic firing (I and II) versus those that do not (III and IV), with frequent mGluR1 expression in the former and rare expression in the latter two classes. This observation is of particular interest in view of previous data indicating that the contribution of mGluRs to excitatory responses is significant only after activation by high-frequency stimuli (Bashir et al., 1993; Miles and Poncer, 1993). The evidence for the preferential extrasynaptic localization of mGluRs (Baude et al., 1993) is also indicative for a functional role of these glutamate receptors under conditions of high-frequency stimulation.

The rhythmic activity induced by mGluR activation in type I and type II interneurons, which is most likely mGluR1-mediated, is independent of the previously reported intracellular Ca^{2+} oscillations, which were shown to be mGluR5-dependent (Kawabata et al., 1996). Hence, one would predict the absence of Ca^{2+} oscillations in type II interneurons because they express mGluR1 only.

The differential expression of mGluR1 and mGluR5 in the four subtypes of interneurons and the associated differences in functional properties allow for several speculations about the functional role of these mGluRs in interneurons. From the present findings, one might infer that the type I and II interneurons will show a rhythmic action potential pattern during excitation. In this way, these neurons will be able to act as "pacemakers" of the excitability of pyramidal cells, depending on the termination of their axons on the pyramidal cell soma–dendrites. In other words, type I and II interneurons might be involved in phase-locking rhythmic activity of pyramidal cell ensembles. Such a role has been proposed previously for somatostatin-positive interneurons (type I interneurons presented here), which innervate the distal dendrites of CA1 pyramidal cells (Katona et al., 1999). The somatostatin-positive interneurons are interesting candidates for governing the time window in which oscillatory activity can take place. Because of the large convergence of many pyramidal cells onto somatostatin-positive interneurons (Ali and Thomson, 1998), these interneurons might sense the electrical activity of a large ensemble of pyramidal cells.

The prominent rhythmic activity induced in somatostatin-positive cells by mGluR1 activation also raises the question whether and under which conditions somatostatin-positive interneurons may control the activity of parvalbumin-positive interneurons in the hippocampus, given that this modulatory activity has been reported recently in somatosensory cortex (Connors et al., 1999). This is an intriguing question in view of previous

findings showing that synchronous firing of many pyramidal cells is initiated by interneurons whose characteristics indicate their parvalbuminergic nature (Cobb et al., 1995). Hence, more detailed studies regarding the target cells whose activity is controlled by somatostatin-positive interneurons are warranted. It is conceivable, however, that somatostatin- and parvalbumin-positive interneurons may be recruited differentially during distinct oscillatory states (e.g., θ vs γ oscillations).

In summary, we have characterized interneurons based on their differential response to type I mGluR activation and have established a correlation between functional, molecular, and morphological properties. We have shown that hippocampal interneurons in the CA1 oriens–alveus region differentially respond to group I mGluR activation and that they display a distinct expression profile of mGluR1 and mGluR5. Of note is the rhythmic activity, induced selectively in type I and type II neurons, which is presumably mGluR1-mediated. It remains to be determined whether mGluR1 activation in type I and II interneurons is critical for the generation of a distinct oscillatory rhythm.

REFERENCES

Ali AB, Thomson AM (1998) Facilitating pyramid to horizontal oriens-alveus interneurone inputs: dual intracellular recordings in slices of rat hippocampus. J Physiol (Lond) 507:185–199.

Bashir ZI, Bortolotto ZA, Davies ZH, Berretta N, Irving AJ, Seal AJ, Henley JM, Jane DE, Watkins JC, Collingridge GL (1993) Induction of LTP in the hippocampus needs synaptic activation of glutamate metabotropic receptors. Nature 363:347–350.

Baude A, Nusser Z, Roberts JDB, Mulvihill E, McIlhinney RAJ, Somogyi P (1993) The metabotropic glutamate receptor (mGluR1α) is concentrated at perisynaptic membrane of neuronal subpopulations as detected by immunogold reaction. Neuron 11:771–787.

Boddeke HWGM, Best R, Boeijinga PH (1997) Synchronous 20 Hz rhythmic activity in hippocampal networks induced by activation of metabotropic glutamate receptors *in vitro*. Neuroscience 76:653–658.

Buhl EH, Halasy K, Somogyi P (1994) Diverse sources of hippocampal unitary inhibitory postsynaptic potentials and the number of synaptic release sites. Nature 368:823–828.

Buzsaki G, Chrobak JJ (1995) Temporal structure in spatially organized neuronal ensembles: a role for interneuronal networks. Curr Opin Neurobiol 5:504–510.

Carment L, Woodhall G, Ouardouz M, Robitaille R, Lacaille JC (1997) Interneuron-specific Ca^{2+} responses linked to metabotropic and ionotropic glutamate receptors in rat hippocampal slices. Eur J Neurosci 9:1625–1635.

Catania MV, Tölle TR, Monyer H (1995) Differential expression of AMPA receptor subunits in NOS-positive neurons of cortex, striatum, and hippocampus. J Neurosci 15:7046–7061.

Cobb SR, Buhl EH, Halasy K, Paulsen O, Somogyi P (1995) Synchronization of neuronal activity in hippocampus by individual GABAergic interneurons. Nature 378:75–78.

Connors B, Beierlein M, Gibson JR (1999) An electrically coupled network of interneurons drives synchronous inhibition in the neocortex. Soc Neurosci Abstr 29:322.

Fisahn A, Pike FG, Buhl EH, Paulsen O (1998) Cholinergic induction of network oscillations at 40 Hz in the hippocampus *in vitro*. Nature 394:186–189.

Freund TF, Buzsáki G (1996) Interneurons of the hippocampus. Hippocampus 6:347–470.

Katona I, Acsády L, Freund TF (1999) Postsynaptic targets of somatostatin-immunoreactive interneurons in the rat hippocampus. Neuroscience 88:37–55.

Kawabata S, Tsutsumi R, Kohara A, Yamaguchi T, Nakanishi S, Okada M (1996) Control of calcium oscillations by phosphorylation of metabotropic glutamate receptors. Nature 383:89–92.

Kawaguchi Y (1997) Selective cholinergic modulation of cortical GABAergic cell subtypes. J Neurophysiol 78:1743–1747.

Kerner JA, Standaert DG, Penny JB Jr, Young AB, Landwehrmeyer GB (1997) Expression of group one metabotropic glutamate receptor subunit mRNAs in neurochemically identified interneurons in the rat neostriatum, neocortex and hippocampus. Brain Res Mol Brain Res 48:259–269.

Lambolez B, Audinat E, Bochet P, Crepel F, Rossier J (1992) AMPA receptor subunits expressed by single Purkinje cells. Neuron 9:247–258.

Lee K, Boden PR (1997) Characterization of the inward current induced by metabotropic glutamate receptor stimulation in rat ventromedial hypothalamic neurones. J Physiol (Lond) 504:649–663.

McBain CJ, DiChiara TJ, Kauer JA (1994) Activation of metabotropic glutamate receptors differentially affects two classes of hippocampal interneurons and potentiates excitatory synaptic transmission. J Neurosci 14:4433–4445.

McMahon LL, Williams JH, Kauer JA (1998) Functionally distinct groups of interneurons identified during rhythmic carbachol oscillations in hippocampus in vitro. J Neurosci 18:5640–5651.

Miles R, Poncer J-C (1993) Metabotropic glutamate receptors mediate a post-tetanic exciation of guinea-pig hippocampal inhibitory neurons. J Physiol (Lond) 463:461–473.

Miles R, Toth K, Gulyas AI, Hajos N, Freund TF (1996) Differences between somatic and dendritic inhibition in the hippocampus. Neuron 16:815–823.

Montminy MR, Goodman RH, Horovitch SJ, Habener JF (1984) Primary structure of the gene encoding rat presomatostatin. Proc Natl Acad Sci USA 81:3337–3340.

Monyer H, Jonas P (1995) PCR analysis of ion channel expression in single neurons of brain slices. In: Single-channel recording (Sakmann B, Neher E, eds), pp 357–373. New York: Plenum.

Nakanishi S, Nakajima Y, Masu M, Ueda Y, Nakahara K, Watanabe D, Yamaguchi S, Kawabata S, Okada M (1998) Glutamate receptors: brain function and signal transduction. Brain Res Brain Res Rev 26:230–235.

Parra P, Gulyás AI, Miles R (1998) How many subtypes of inhibitory cells in the hippocampus? Neuron 20:983–993.

Sik A, Penttonen M, Ylinen A, Buzsáki G (1995) Hippocampal CA1 interneurons: an *in vivo* intracellular labeling study. J Neurosci 15:6651–6665.

Singer W (1993) Synchronization of cortical activity and its putative role in information processing and learning. Annu Rev Physiol 55:349–374.

Staub C, Vranesic I, Knöpfel T (1992) Responses to metabotropic glutamate receptor activation in cerebellar Purkinje cells: induction of an inward current. Eur J Neurosci 4:832–839.

Stuart GJ, Dodt HU, Sakmann B (1993) Patch-clamp recordings from the soma and dendrites of neurons in brain slices using infrared video microscopy. Pflügers Arch 423:511–518.

Traub RD, Whittington MA, Colling SB, Buzsáki G, Jefferys JG (1996) Analysis of gamma rhythms in the rat hippocampus *in vitro* and *in vivo*. J Physiol (Lond) 493:471–484.

Traub RD, Jefferys JG, Whittington MA (1997) Simulation of gamma rhythms in networks of interneurons and pyramidal cells. J Comput Neurosci 4:141–150.

Whittington MA, Traub RD, Jefferys JG (1995) Synchronized oscillations in interneuron networks driven by metabotropic glutamate receptor activation. Nature 373:612–615.

Whittington MA, Stanford IM, Colling SB, Jefferys JG, Traub RD (1997) Spatiotemporal patterns of γ frequency oscillations tetanically induced in the rat hippocampal slice. J Physiol (Lond) 502:591–607.

Woodhall G, Gee CE, Robitaille R, Lacaille JC (1999) Membrane potential and intracellular Ca^{2+} oscillations activated by mGluRs in hippocampal stratum oriens/alveus interneurons. J Neurophysiol 81: 371–382.